The Egyptian Journal of Radiology and Nuclear Medicine (2011) **42**, 57–67

Egyptian Society of Radiology and Nuclear Medicine

The Egyptian Journal of Radiology and Nuclear Medicine

www.elsevier.com/locate/ejrnm
www.sciencedirect.com

Role of FIESTA combined with conventional MRI in the evaluation of traumatic brachial plexus roots injury

Sabry A. El Mogy [a,*], Jehan A. Mazroa [a,1], Mahamad Kassem [a,2], Mohamed S. El Mogy [b,3], Ibraheem S. El Mogy [b,4]

[a] *Faculty of Medicine, Mansoura University, Egypt*
[b] *Fellow Ship Ministry of Health, Mansura, Egypt*

Received 19 October 2010; accepted 10 January 2011
Available online 26 March 2011

KEYWORDS
Brachial plexus root injury;
FIESTA;
Imaging of brachial plexus

Abstract *Purpose:* Purpose was to evaluate the role of Fast imaging employing steady-state acquisition (FIESTA) together with conventional MR sequences in the evaluation of traumatic brachial plexus roots injury compared to post contrast MR and Spin Echo MR myelographic studies.
Patients and methods: In this prospective study, 16 patients with a mean age of 17.9 y who presented with traumatic brachial plexus roots injury in motor cycle and car accidents were studied with FIESTA, conventional MR, post contrast MR and MR myelography sequences. Imaging findings included: pseudo-meningocele/hemorrhage near the nerve root exit, failure of visualization of

Abbreviations: BPI, brachial plexus injury; FIESTA, Fast imaging employing steady-state acquisition; SSFP, steady state free precision; IVF, inter vertebral foramen; MRM, magnetic resonance myelography; SE, Spin Echo

* Corresponding author. Mobile: +20 110607830.
E-mail addresses: drsabryelmogy@Yahoo.com (S.A. El Mogy), jehanras@hotmail.com (J.A. Mazroa), okassem2000@Yahoo.com (M. Kassem), dr_m_sabry@Yahoo.com (M.S. El Mogy), imogy@hotmail.com (I.S. El Mogy).
[1] Mobile: +20 160338481.
[2] Mobile: +20 106070620.
[3] Mobile: +20 110607827.
[4] Mobile: +20 104848252.

Peer review under responsibility of Egyptian Society of Radiology and Nuclear Medicine.
doi:10.1016/j.ejrnm.2011.02.001

Production and hosting by Elsevier

the nerve root (dorsal, ventral or both), retracted avulsed nerve root ends, spinal cord edema, and para spinal muscles edema and hemorrhage. Diagnostic accuracy was calculated for each MR sequence. Imaging findings were compared with the gold standard operative findings.

Results: FIESTA combined with conventional MR depicted pseudomeningoceles, non visualized nerve roots, cord displacement, and para spinal muscles abnormalities in 15 patients (93.8%), cord edema in four patients (25%). Pre and post contrast MR detected pseudomeningoceles and non visualized nerve roots in 13 patients (81.3%) while Spin Echo myelography detected pseudomeningoceles and non visualized nerve roots in 14 patients (87.5%). FIESTA combined with conventional MR showed the highest diagnostic accuracy (93.8%) compared to pre and post MR (81.3%) and Spin Echo myelography (87.5%).

Conclusion: It is crucial to differentiate between preganglionic and postganglionic injuries for optimal treatment planning in patients with BPI. Conventional MR imaging yielded suboptimal information regarding the fine details of nerve roots' injury. MR myelography showed some artifacts that decreased overall diagnostic accuracy, FIESTA combined with conventional MR depicted nerve segments in greater detail and provided important information about the relationship of the nerves to nearby structures, it provided high contrast resolution between cerebrospinal fluid and solid structures, allowing the reconstruction of elegant multi-planar images that highlight the injured nerves. Contrast study is recommended in mild trauma cases with normal morphological study.

1. Introduction

Brachial plexus injury (BPI) is a severe neurological injury that causes functional impairment of the affected upper limb. Brachial plexus is formed from C5, C6, C7, C8, and T1 nerve roots. There may be contributions from C4, and T2. A plexus with contributions from C4 is called "prefixed" {28–62%}. "Postfixed" = contributions from T2 {16–73%} (1–3).

The most common cause of BPI is traffic accidents (especially motorcycle accidents). The other common cause of BPI is birth palsy. The majority of obstetric BPI involves the upper brachial plexus and is referred to as Duchenne-Erb's palsy. Lower type obstetric BPI (Klumpke's palsy) is rare. Other traumatic causes include accidents at work, sports injuries, incised wounds, gunshot wounds, carrying a heavy object, and patient mal-positioning during surgery. Tumors, irradiation, and congenital abnormalities such as cervical ribs can be non traumatic causes of brachial plexopathy (4–7).

Table 1 Showed clinical information of the patients.

Gender	Male	Female
No. (%)	13 (81%)	3 (19%)
Side	Right	Left
No. (%)	11 (67%)	5 (33%)
Age	23.68 ± 10.39 y	
Mean ± SD		
(Min–Max)	(9 months to 36 y)	

Brachial plexus is divided into *roots* (originates from the cord, pass through inter-vertebral foramins), *trunks* (at lateral border of middle scalene muscle at scalene muscles triangle), *divisions* (infra clavicular), *cords* (lateral to the first rib), and *branches*. Preganglionic injury = spinal roots are avulsed from the spinal cord; loss of motor function. Treatment = neurotization (nerve transfer). Postganglionic injury = distal to the dorsal root ganglion; loss of motor and sensory function. Treatment = surgical repair/grafting (6,8,9).

Imaging studies play an essential role in differentiating preganglionic injuries from postganglionic lesions, a differentiation that is crucial for determining the management of BPI (10). With respect to preganglionic injuries, functions of some denervated muscles are restored with nerve transfers (neurotization). Post ganglionic lesions are repaired with nerve grafting or followed up conservatively (in nerve stretching). In nerve transfer, donor nerves are attached to the ruptured distal stump, scarifying the original function of the nerve for more beneficial results in the upper limb. It is generally agreed that the top priority of nerve repair is restoration of biceps muscle function (elbow flexion) and shoulder function. Intercostal nerves are commonly used as the donor nerves (11).

Fast imaging employing steady-state acquisition (FIESTA) is one of the steady-state coherent imaging sequences, and its signal is related to the ratio of T2 to T1. FIESTA achieves a high contrast-to-noise ratio with fewer flow artifacts; thus, this sequence is suitable for MR myelography. The use of 3D FIESTA, enable acquisition of thin slices, it provides submillimetric spatial resolution and high contrast resolution between

Table 2 Showed MRI findings (conventional and FIESTA) in our patients.

Findings Sequences	Pseudo-meningocele	Non visualized nerve root	Cord displacement	Cord edema	Para spinal muscle abnormalities (Hge/edema/enhancement)
FIESTA + non contrast MR	15 (93.8%)	15 (93.8%)	15 (93.8%)	4 (25%)	15 (93.8%)
Pre + post contrast MR	13 (81.3%)	13 (81.3%)	15 (93.8%)	4 (25%)	15 (93.8%)
Non contrast MR + SE myelography	14 (87.5%)	14 (87.5%)	15 (93.8%)	4 (25%)	15 (93.8%)

Table 3 Showed diagnostic accuracy of the three MR sequences regarding the first two signs.

MR sequences	FIESTA + non contrast conventional MRI	Pre + post contrast MRI	MR myelography
Diagnostic accuracy	93.8%	81.3%	87.5%

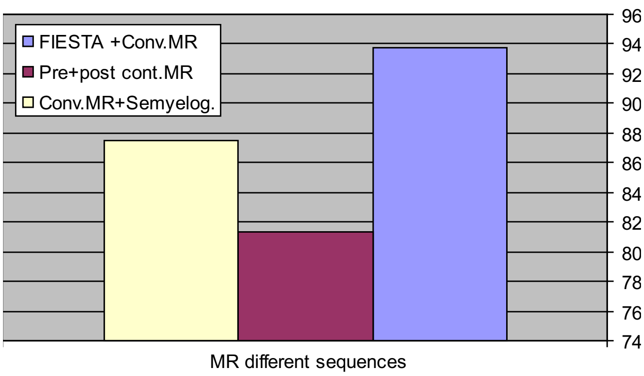

Graph 1 Showing the diagnostic accuracy of the three MR sequences regarding the first two signs.

cerebrospinal fluid and solid structures, allowing the reconstruction of elegant multiplanar images that highlight the course of each cranial and spinal nerve (12–16).

The radiological signs of brachial plexus roots' injury are: (a) signal changes in the spinal cord near the nerve root exit, (b) bleeding near the nerve root exit, (c) failure of visualisation of the nerve root (dorsal, ventral, or both), (d) discontinuity in the course of the nerve root, (e) CSF leakage along the nerve root, (f) pseudo-meningocele and (g) para spinal muscles edema/hemorrhage/enhancement (17,10,18).

Aim of the work was to evaluate the role of Fast imaging employing steady-state acquisition (FIESTA) together with conventional MR sequences in evaluation of traumatic brachial plexus roots' injury compared to post contrast MR and Spin Echo MR myelographic studies.

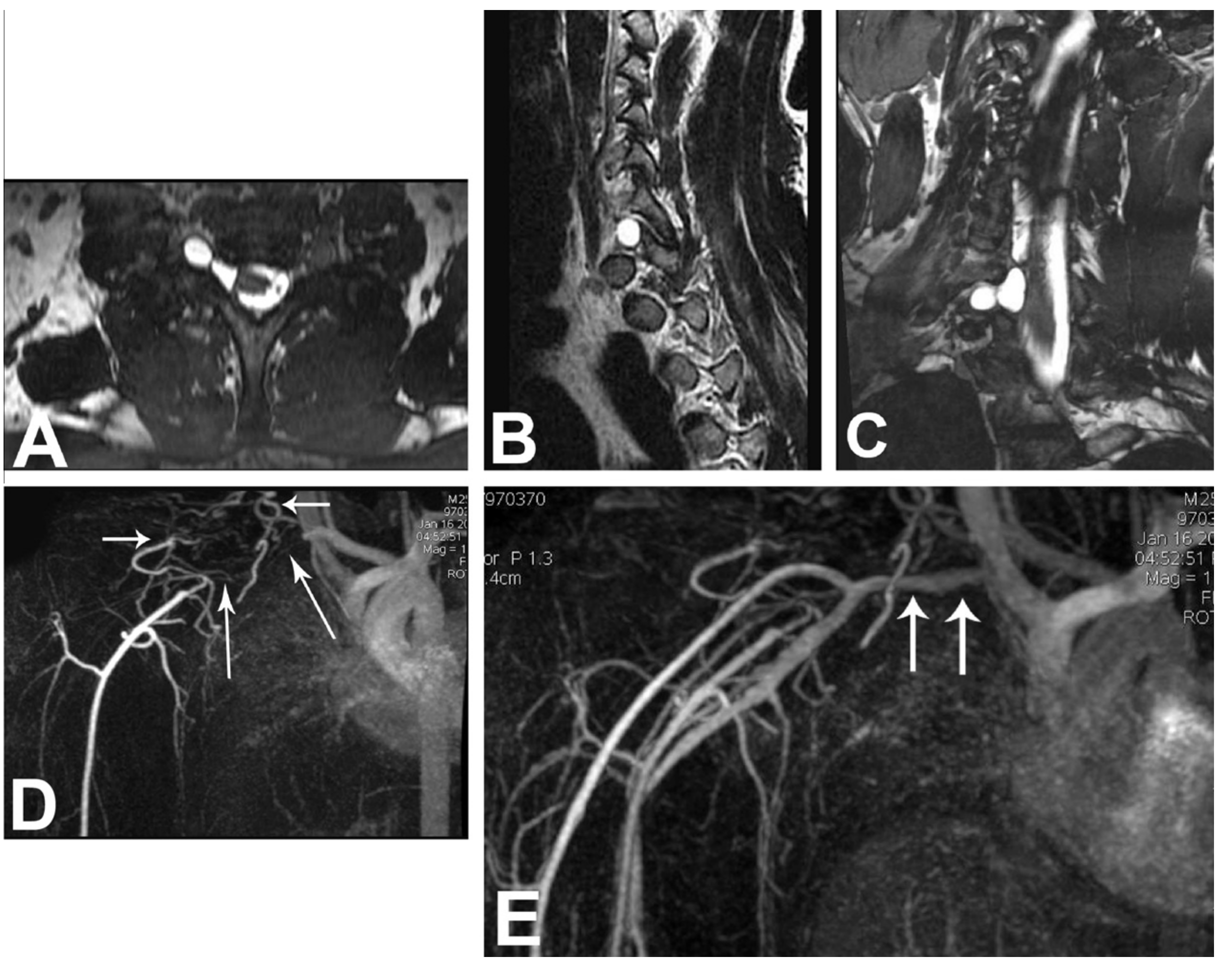

Fig. 1 A case of RT.C7 spinal nerve root injury with pseudo-meningoceles formation and traumatic rupture of RT.Subclavian artery. Male patient aged 26 y with a history of car accident. (A) Axial T2FSE showing RT.sided pseudomeningocele at C7 spinal nerve protruding from the intervertebral foramen. (B) Sagittal T2FSE showing RT.sided pseudo-meningocele at the intervertebral foramen. (C) 3D FIESTA clearly shows RT.sided pseudomeningocele at C7 spinal nerve. (D) Contrast enhanced TOF MRA showing complete tear of RT.Subclavian artery (long arrows) with collateral formation (short arrows). (E) MRV PC showing normal appearance of RT.Subclavian vein (arrows).

2. Patients and methods

This prospective study conducted at a private center in Mansoura, Egypt from June 2009 till November 2010 contained 16 patients with brachial plexus roots' injury (11 RT.sided, 5 LT.sided), their ages ranged from 8 months to 35 y with a mean of 17.9 y. All patients had a history of motorcycle or car trauma, there were 13 male and three females. Patients referred from emergency and neurosurgical units of both the pediatric hospital and the main hospital of Mansoura Univer-

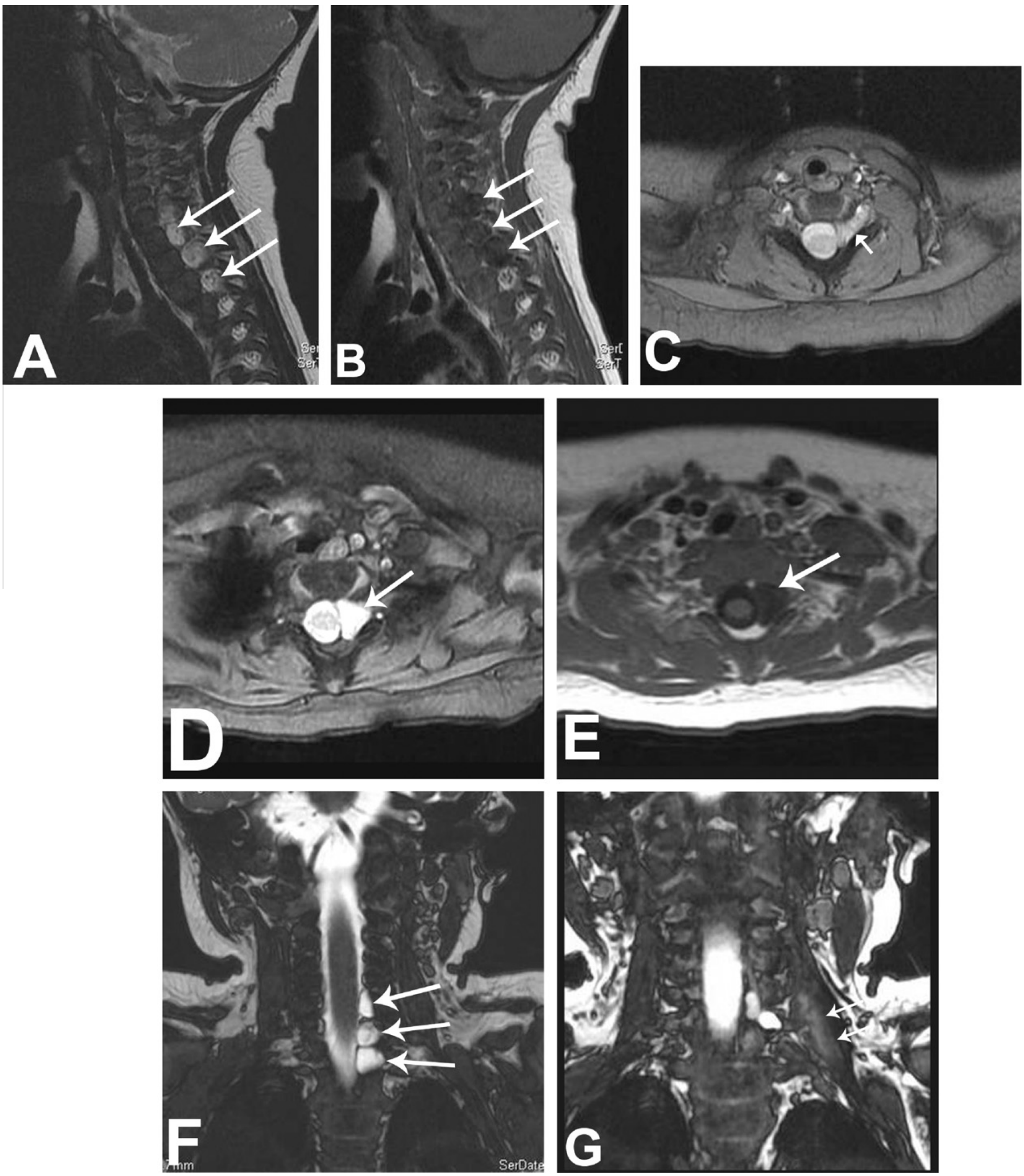

Fig. 2 A case of LT. C5, C6, C7 spinal nerves root injury with pseudo-meningocele formation. Male infant aged 0.8 y with history of car accident. (A) Sagittal T2 FSE and (B) sagittal T1 FSE showing three LT.sided pseudomeningoceles at C5, C6 and C7 spinal nerves protruding from intervertebral foramen (arrows). (C) Axial GRE at C5 level and (D) Axial GRE at C6 level. Showing cord displacement, LT. pseudomeningoceles and non visualized LT. nerve roots. (E) Axial T1FSE and at C6 level showing cord displacement and C6 spinal nerve pseudo-meningocele (arrow). (F and G) 3D FIESTA showing C5, C6, C7 pseudo-meningoceles (long arrows) and edema of LT. multifidus and erector spinea muscles at a posterior level (short arrow).

sity after meticulous clinical examination by the neurosurgeon were suspected to have brachial plexus roots' injury.

Clinical findings which suggest preganglionic BPI are: (1) Horner's syndrome, (2) paralysis of serratus anterior muscle which causes winging of the scapula and (3) paralysis of rhomboids muscles which causes lateral deviation of the scapula.

Electrodiagnostic studies of root avulsion:

- EMG changes after 3 weeks from the injury.
- Normal Sensory nerve Action Potential (SNAP).
- Absent Somato-sensory Evoked Potential (SEP).
- Denervation of cervical para spinal muscles. Spontaneous activity and complete absence of voluntary motor units in muscles innervated by the injured root.

Written consent was obtained from adult patients or parents of infants and pediatric patients.

Pediatric patients receive sedation (chloral hydrate) by an anesthetist in a dose of 0.5 ml/kg BW.

Patients performed MRI using GE 1.5 T medical system. Sequences obtained were the following: GRE scout (axial, coronal, sagittal), sagittal T2 FSE, Sagittal T1 FSE, Axial

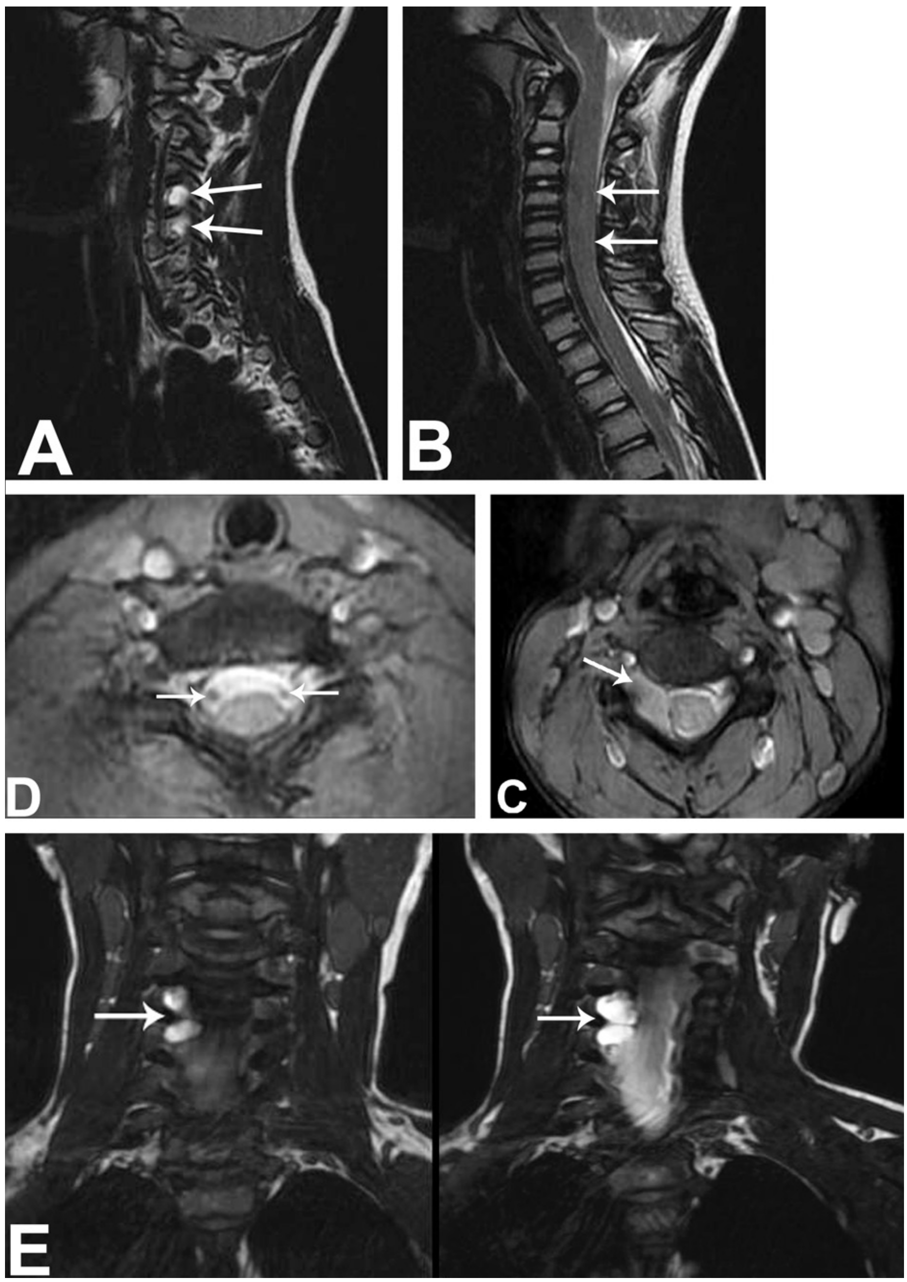

Fig. 3 A case of RT.C4, C5 spinal nerves root injury with pseudo-meningocele formation. Male child aged 9 y with history of motorcycle accident. (A) Sagittal T2FSE (RT.para sagittal view), (B) Sagittal T2FSE (mid sagittal view) revealed pseudo-meningocele at RT.C4, C5 spinal nerve (long arrows) with cord swelling, edema and contusion (short arrows). (C) Axial GRE; revealed absence of RT.C4 nerve root with pseudo-meningocele (long arrow), (D) axial GRE at the normal C6 level showing intact nerve roots bilaterally (short arrows). (E) 3D FIESTA: revealed pseudo-meningocele at RT.C4, C5 nerve roots.

GRE, axial T1FSE, 3D FIESTA myelogram, SE myelogram and post contrast axial, coronal, and sagittal T1WIs.

Parameters of conventional MRI were:

Sagittal T2FSE: TR/TE: 2000/114–117 and FOV: 18×18–24×24 and 3 mm thickness and NEX: 2 and matrix: 320×224.
Sagittal T1FSE: TR/TE:520–560/9–10 and FOV: 24×24 and NEX: 2 and matrex: 320×192 and 3 mm thickness.
Axial GRE: TR/TE: 417–524/3–16 and FOV: 20×16–23×18.4 and 4 mm thickness and NEX: 2 and matrex: 320×224.
Axial T1FSE: TR/TE: 820/9.6 and FOV: 20×20 and 3 mm thickness and NEX: 2 and matrex: 320×192.
Spin Echo myelography: TR/TE: 2997/1202 and FOV: 24×24 and 40 mm thickness and 2 mm overlap and NEX: 0.89 and matrex: 320×256.

Parameters of FIESTA were: TR/TE: 6.4–9.3/2.4–2.7 and FOV: 17×17–22×22 and NEX: 2 and matrex: 320×192 and thickness: 2–2.7 mm and overlap: 1.5 mm. Acquisition time: 3.30–4.30 min.

Post contrast studies were performed for all patients using Gadolinium in a dose 0.1 mmol/kg body weight, which was administered intravenously via an injection system at a rate of 1 mL/s.

Patients were scanned within 2 weeks from the injury (mean 7 days) to avoid muscles changes (atrophy).

Our study focused on the root injury, other parts of brachial plexus injury (including trunks, divisions, cords, branches) were excluded from our study.

Approval of the ethical committee was taken. All patients underwent surgical nerve root repair (neurotization: transfer of intercostals nerve), radiological findings were compared with operative findings.

3. Statistical analyses

The statistical analysis of data was done by using EXCEL program and SPSS (SPSS, Inc., Chicago, IL) program statistical package for social science version 16.

The description of the data done in the form of mean ± SD for quantitative data and frequency and proportion for qualitative data.

The analysis of the data was done to test statistical significant difference between groups.

Paired sample *t*-test was used to compare one group at different times.

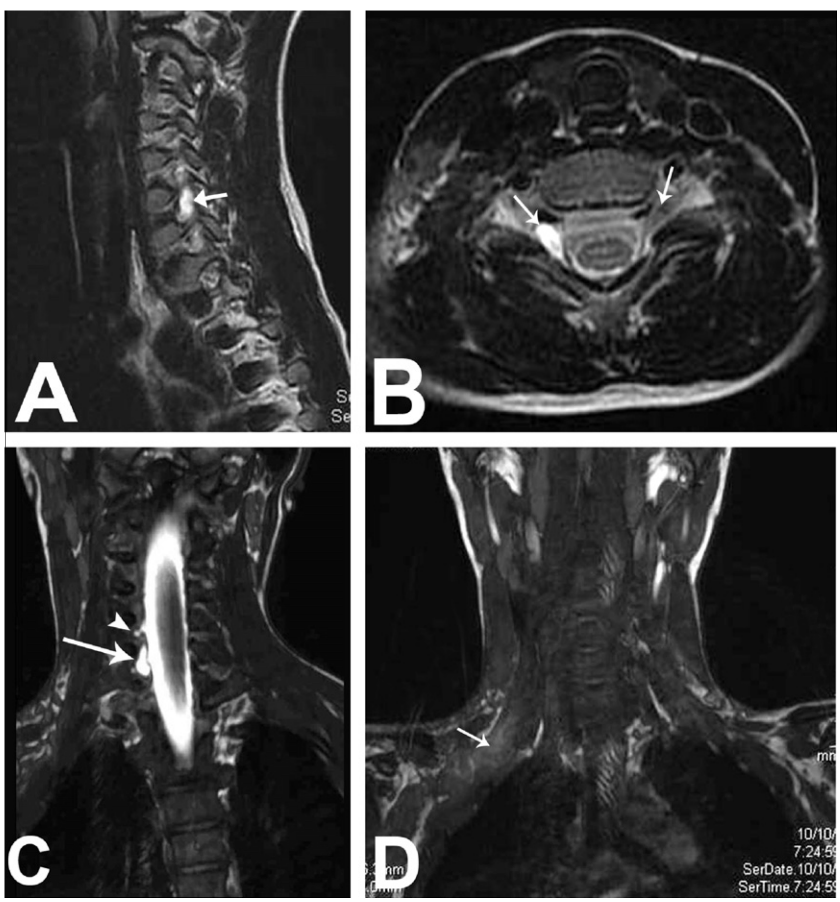

Fig. 4 A case of RT.C5 spinal nerve root injury with pseudo-meningocele formation. Male patient aged 31 with history of car accident. (A) Sagittal T2FSE showing RT.C5 pseudo-meningocele protruding from intervertebral foramen. (B) Axial GRE showing RT.C5 pseudo-meningocele (long arrow), note intact LT. nerve root (short arrow). (C) 3D FIESTA showing RT.C5 pseudo-meningocele (long arrow). (D) 3D FIESTA showing edema and hematoma of RT.multifidus, erector spinea muscles (short arrow). Note small RT.C4 pseudo-meningocele consistent with partial nerve root avulsion (arrow head).

Chi square test was used for qualitative data.

N.B: P is significant if $\leqslant 0.05$ at confidence interval 95%.

4. Results

Our study contained 16 patients with traumatic brachial roots' injury caused by motor cycle or car injuries, 11 were RT.sided, 5 were LT.sided, clinically all showed root injury (also in MRI). Clinical information of our patients was summarized in Table 1.

Findings of brachial plexus root injury were: pseudomeningocele, non visualized nerve root, retracted avulsed root, cord displacement, cord edema and hemorrhage, and para spinal muscle edema/hemorrhage.

FIESTA combined with conventional non contrast MR detected pseudomeningocele in 15 patients, non visualized nerve roots in 15 patients, cord displacement in 15 patients, cord edema in 4 patients, para spinal muscle edema and hemorrhage in 13 patients.

Pre and post contrast MR detected pseudomeningocele in 13 patients, non visualized nerve roots in 13 patients, cord displacement in 13 patients, cord edema in four patients, para spinal muscle edema and enhancement (which denotes muscle denervation and dysfunction) in 13 patients.

Conventional non contrast MR combined with SE myelography detected pseudomeningocele in 14 patients, non visualized nerve roots in 14 patients, cord displacement in 13 patients, cord edema in four patients, para spinal muscle edema and hemorrhage in 13 patients.

FIESTA sequence yielded highest diagnostic accuracy of pseudomeningocele detection (93.8%) compared to pre + post contrast MR (81.3%) and non contrast MR + SE myelogram (87.5%).

FIESTA sequence yielded highest diagnostic accuracy of non visualization of nerve roots (93.8%) compared to pre + -post contrast MR (81.3%) and non contrast MR + SE myelogram (87.5%).

The three imaging sequences yielded the same accuracy regarding cord displacement (39.8%), cord edema (25%), and para spinal muscles edema/hemorrhage (93.8%). These radiological findings were shown at Table 2.

Over all diagnostic accuracy of the three imaging sequences regarding the most important signs of brachial plexus roots injury (which are pseudomeningoceles + non visualized nerve roots) are shown in Table 3 and Graph 1.

5. Discussion

A brachial plexus lesion involving spinal nerves C5 and C6 leads to paralysis of the shoulder muscles and biceps. When the damage extends to the spinal nerve C7, some of the wrist muscles are also impaired, when damage involves C8 and T1 leads to paralysis of the fore arm flexor and the intrinsic muscles of the hand. Avulsion of the T1 root (a pre-ganglionic in-

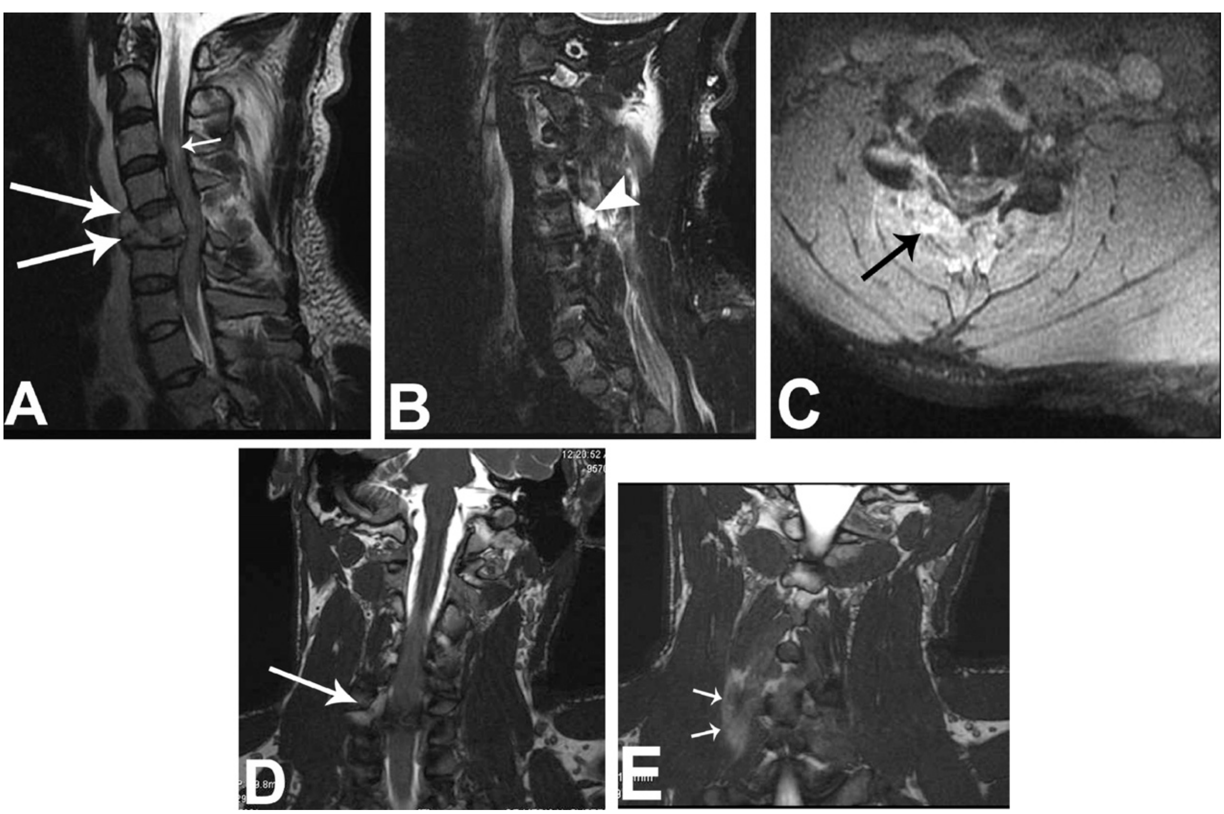

Fig. 5 A case of fractured C5 with RT.C5 spinal nerve root injury and pseudo-meningocele formation. Male patient aged 34 y with history of car accident. (A) Sagittal T2FSE showing fracture and posterior dislocation of C5 vertebra (long arrows) with cord contusion (short arrow). (B) RT.para sagittal view showing C5 pseudo-meningocele (arrow head). (C) Axial GRE showing fractured C5 vertebra compressing the cord with edema and hematoma of multifidus and erector spinea muscles (long arrow). (D) 3D FIESTA revealed RT.C5 pseudo-meningocele (long arrow). (E) 3D FIESTA revealed edema and hematoma of para spinal muscles (short arrows).

jury) interrupts the T1 sympathetic ganglion, causing Horner's syndrome [miosis, enophthalmos, ptosis, and anhydrosis] (19,11).

Patients with severe BPI should undergo an appropriate reconstructive procedure before denervated muscle become irreversibly atrophic and they are no longer good candidates for primary nerve repair (17).

Imaging studies play an essential role in differentiating between preganglionic and postganglionic injuries, a distinction that is crucial for optimal treatment planning. False negative findings in cases of partial root avulsion, intradural fibrosis, artifacts caused by: respiratory movements of the chest, swallowing movements of the hypopharynx and larynx, and flow in the cervical vessels (12,13,20–23).

MR myelography provides good images for the thecal sac, it's disadvantages are CSF and patients' movements artifacts, the inclusion of vertebral arteries and spinal venous plexus, difficulty of determination of exact injury level (17).

New imaging techniques including FIESTA sequence, diffusion-weighted neurography, and Bezier surface reformation CT can also be useful in the evaluation and management of BPI. Bezier surface reformation allows the depiction of entire intradural nerve roots on a single image. Diffusion-weighted neurography is a cutting-edge technique for visualizing postganglionic nerve roots, but lack depiction of cervical nerves above the level of the C5 nerve (24–27).

Steady state free precession (SSFP) sequences are gradient-echo sequence with small flip angle and short relaxation time. The clinical utility of an SSFP sequence lies in its ability to generate a strong signal in tissues that have a high T2:T1 ratio, such as cerebrospinal fluid (CSF) and fat. SSFP sequences are particularly useful for visualizing the cisternal segments of cranial nerves and spinal nerves because they provide excellent contrast resolution between CSF and nerves, as well as high spatial resolution with sub-millimetric section thicknesses. Another advantage is that the total acquisition time with SSFP sequences is shorter than that with traditional MR imaging pulse sequences, helping to reduce CSF pulsation artifact (25–27). The disadvantages of SSFP imaging include reduced contrast resolution between different soft tissues. In addition, global landmarks may be poorly depicted because of the sub-millimetric section thicknesses. Thus, SSFP sequences play a supplemental role alongside traditional sequences in MR imaging of the cranial and spinal nerves (27–30).

A post traumatic pseudo-meningocele is a valuable sign of a preganglionic lesion, although it is not pathognomonic. Nerve root avulsion commonly occurs without a meningocele, and a meningocele occasionally exits without nerve root avulsion. Absence of roots is also an important sign in detecting a preganglionic lesion (17).

In our study, FIESTA combined with conventional MR imaging detected 15 patients with pseudomeningoceles

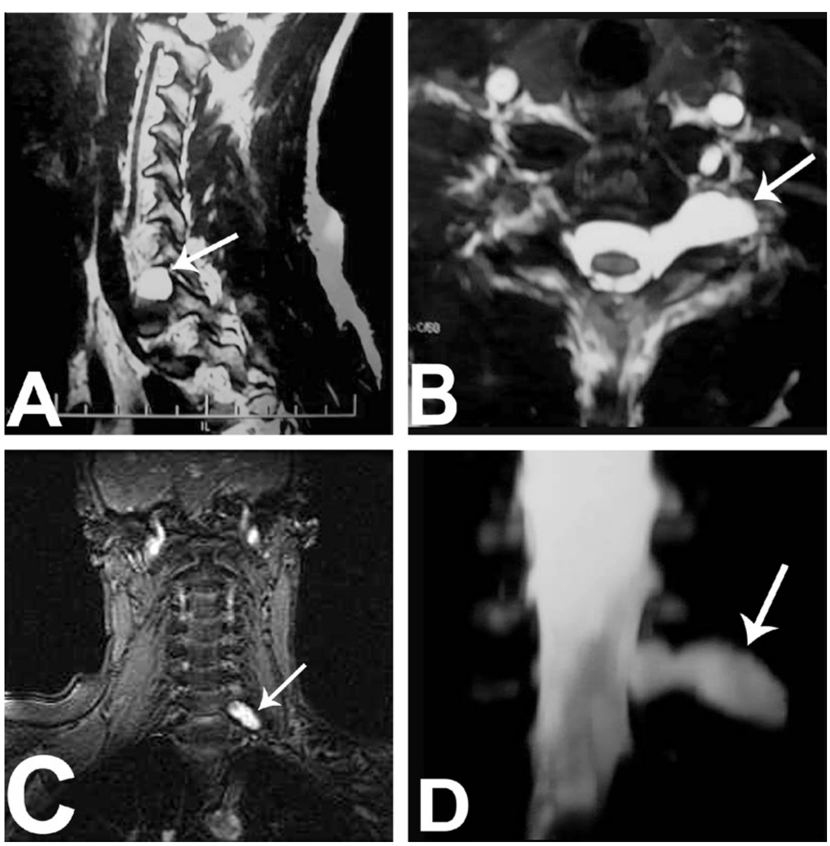

Fig. 6 A case of LT.C7 spinal nerve root injury with pseudo-meningocele formation Male patient aged 20 y with history of motorcycle accident. (A) Sagittal T2FSE revealed pseudo-meningocele at LT.C7 nerve root protruding from the intervertebral foramen (arrow). (B) Axial GRE image showing absent LT. C7 nerve root with pseudo-meningocele (arrow). (C) 3D FIESTA revealed LT.C7 pseudo-meningocele (arrow). (D) SSF FSE myelogram showing LT.C7 pseudo-meningocele (arrow).

(93.8%). Pre and post contrast MR detected 13 patients with pseudomeningoceles (81.3%) and SE myelography detected 14 patients with pseudomeningoceles (87.5%). Pseudomeningoceles were single or multiple at the trauma side (Figs. 1–6).

Signal intensity changes are observed in the spinal cord in approximately 20% of patients with preganglionic injuries. Hyperintense areas on T2-weighted images suggest edema in the acute phase and myelomalacia in the chronic phase. Hypointense lesions on T2-weighted images reflect hemosiderin deposition on account of hemorrhage. Signal intensity changes are either extensive in the affected side of the spinal cord or confined to the exit zone of the ventral nerve root (5,17).

Our study revealed cord edema in 4 patients (25%) detected by all the three MR sequences: FIESTA combined with conventional MR, pre and post contrast MR and SE myelography (Table 2).

Abul-Kasim et al., 2010 (1) reported other radiological findings of brachial plexus nerve roots injury: failure of visualization of the nerve root (dorsal, ventral or both), discontinuity in the course of the nerve root and CSF leakage along the nerve root.

Our study revealed non visualized nerve roots in 15 patients detected by FIESTA combined with conventional imaging (93.8%). Pre and post contrast MR detected 13 patients with non visualized nerve roots (81.3%) and SE myelography detected 14 patients with non visualized nerve roots (87.5%).

Cord displacement was seen in 15 patients (93.8%) detected by all the three MR sequences: FIESTA combined with conventional MR, pre and post contrast MR and SE myelography (Table 2).

Enhancement of intra-dural nerve roots and root stumps suggests functional impairment of nerve roots despite morphologic continuity. Abnormal enhancement of para spinal muscles is an accurate indirect sign of root avulsion injury. Denervated muscles show enhancement as early as 24 h after a nerve is injured. Abnormal enhancement in the multifidus muscle is the most accurate of all para spinal muscle findings, since the multifidus muscle is innervated by a single nerve root (17).

In our study, 15 patients (93.8%) showed para spinal muscle enhancement (at the trauma side) detected in the post contrast MR study.

Our study revealed one patient with mild trauma that showed normal non contrast MR study, didn't show meningocele and showed mild para spinal muscle enhancement (due to mild denervation caused by mild nerve roots stretching instead

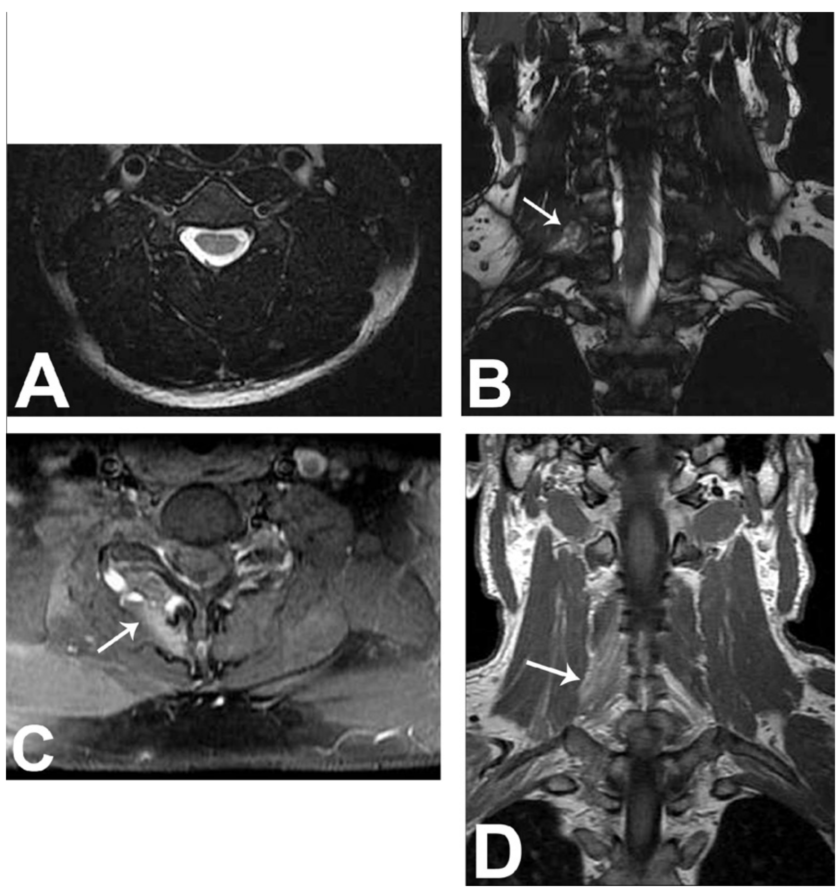

Fig. 7 A case of RT.C7 spinal nerve root stretching without pseudo-meningocele formation showing para spinal muscle edema and enhancement caused by muscle dysfunction. Male patient aged 32 y with history of car accident. (A) Axial T2FSE at level C7 showing normal morphological appearance. (B) Coronal FIESTA showing mild RT.para spinal muscles edema (arrow). (C and D) post contrast axial T1WI (fat suppression) and coronal T1WI showing enhancement of RT.multifidus muscle due to nerve stretching leading to muscle dysfunction (arrows).

of rupture), this is in agreement with previous authors about value of contrast in clinically suspected patients with morphologically normal MR study (Fig. 7).

Doi et al. (22) reported a success rate of MR of about 97% using overlapping or ''fast spin-echo'' MR imaging, while myelography had a success rate of 100%. Nakamura et al. (1997) reported that MRM has sensitivity, specificity and accuracy in detecting Pseudo-meningocele of 88%, 100%, 98%, respectively, and in detecting complete root avulsion of 91%, 92%, 92%. MRM is non-invasive, relatively quick, requires no contrast, provides imaging in multiple projections, and is comparable in diagnostic ability to conventional myelography and CTM.

Hatipoğlu et al., 2007 concluded that 3D FIESTA sequences are superior to SE myelography. FIESTA images can be obtained in a shorter time with sub-millimeter thickness thus CSF pulsation and magnetic susceptibility artifacts decrease. Therefore, 3D FIESTA sequences can be used for obtaining MR cisternography, myelography images for visualization of the cranial and spinal nerves with better resolution (see Fig. 8).

Our study revealed 93.8% diagnostic accuracy in FIESTA for the most specific signs of traumatic plexus roots injury (pseudomeningoceles and non visualized nerve roots) compared to 81.3% for pre and post contrast MR and 87.5% for SE myelography (Table 3 and Graph 1).

Limitations of the FIESTA sequence includes: global landmarks may be poorly depicted because of the sub-millimetric section thicknesses. Thus, SSFP sequences play a supplemental role alongside traditional sequences in MR imaging of the cranial and spinal nerves (17,23).

In our study, the combination of FIESTA with conventional MR sequences yielded the highest diagnostic accuracy compared with other MR sequences.

Every study has some limitations, our own limitations were: (1) limited number of cases and (2) retracted roots stump were not seen due to presence of pseudomeningoceles in 15 patients obscuring avulsed nerve roots.

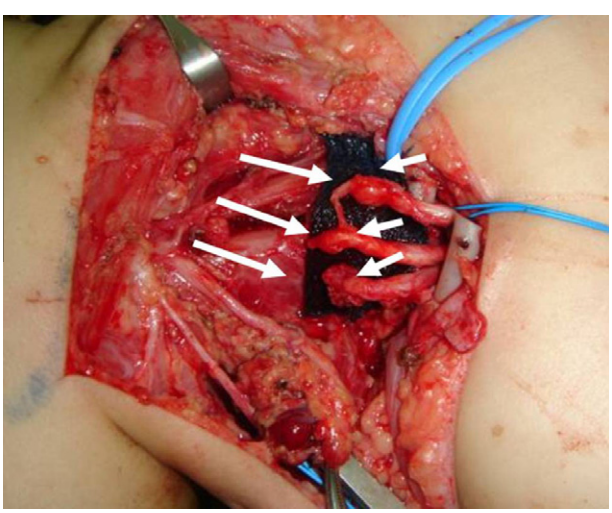

Fig. 8 Showing intra operative repair of preganglionic injury, incision at supra clavicular region showing three avulsed nerve roots (white long arrows) and the ganglia appears distal to the injury (white short arrows).

6. Conclusion

It is crucial to differentiate between preganglionic and postganglionic injuries for optimal treatment planning in patients with BPI. Conventional MR imaging yielded suboptimal information regarding the fine details of nerve roots' injury. MR myelography showed some artifacts that decreased overall diagnostic accuracy, FIESTA combined with conventional MR depicted nerve segments in greater detail and provided important information about the relationship of the nerves to nearby structures, it provided-submillimetric spatial resolution and high contrast resolution between cerebrospinal fluid and solid structures, allowing the reconstruction of elegant multiplanar images that highlight the injured nerves. Contrast study is recommended in mild trauma cases with a normal morphological study.

References

(1) Abul-Kasim Kasim, Backman Clas, Björkman Anders, Dahlin Lars B. Advanced radiological work-up as an adjunct to decision in early reconstructive surgery in brachial plexus injuries. J Brachial Plexus Peripher Nerve Inj 2010;5:14.

(2) Songcharoen P. Management of brachial plexus injury in adults. Scand J Surg 2008;97(4):317–23.

(3) Wiberg M, Backman C, Wahlstrom P, Dahlin LB. Brachial plexus injuries in adults. Early reconstruction for better clinical results. Lakartidningen 2009;106(9):586–90.

(4) Van Es HW. MRI of the brachial plexus. Eur Radiol 2001;11(2):325–36.

(5) Bhandari PS, Sadhotra LP, Bhargava P, Bath AS, Mukherjee MK, Pauline Babu MS. Current trends in the management of brachial plexus injuries. Indian J Neurotrauma (IJNT) 2008;5(1):21–5.

(6) Terzis Julia K, Papakonstantinou Konstantinos C. The surgical treatment of brachial plexus injuries in adults. Plast Reconstr Surg 2000;106(5):1097–124.

(7) Narakas AO. The treatment of brachial plexus injuries. Int Orthop 1985;9(1):29–36.

(8) Castillo Mauricio. Imaging the anatomy of the brachial plexus: review and self-assessment module. AJR 2005;185.

(9) Belzberg AJ, Dorsi MJ, Storm PB, Moriarity JL. Surgical repair of brachial plexus injury: a multinational survey of experienced peripheral nerve surgeons. J Neurosurg 2004;101:365–76.

(10) Hayashi N, Yamamoto S, Okubo T, et al.. Avulsion injury of cervical nerve roots: enhanced intradural nerve roots at MR imaging. Radiology 1998;206:817–22.

(11) Belzberg AJ, Dorsi MJ, Storm PB, Moriarity JH. Surgical repair of brachial plexus injury: a multinational survey of experienced peripheral nerve surgeons. J Neurosurg 2004;101:365–76.

(12) Rankine JJ. Adult traumatic brachial plexus injury. Clin Radiol 2004;59:767–74.

(13) Todd M, Shah GV, Mukherji SK. MR imaging of brachial plexus. Top Magn Reson Imaging 2004;15:113–25.

(14) Hatipoğlu Hatice Gul, Durakoğlugil Tuğba, Cılız Deniz, Yuksel Enis. Comparison of FSE T2W and 3D FIESTA sequences in the evaluation of posterior fossa cranial nerves with MR cisternography. Diagn Interv Radiol 2007;13:56–60.

(15) Takahara T, Hendrikse J, Yamashita T, Mali WP, Kwee TC, Imai Y, Luijten PR. Diffusion-weighted MR neurography of the brachial plexus: feasibility study. Radiology 2008;249(2):653–60.

(16) Bertelli JA, Ghizoni MF. Reconstruction of C5 and C6 brachial plexus avulsion injury by multiple nerve transfers: spinal accessory to suprascapular, ulnar fascicles to biceps branch, and triceps long or lateral head branch to axillary nerve. J Hand Surg 2004;29:131–9.

(17) Yoshikawa Takeharu, Hayashi Naoto, Yamamoto Shinich, Tajiri Yasuhito, Yoshioka Naoki, Masumoto Tomohiko, Mori Harushi, Abe Osamu, Aoki Shigeki, Ohtomo Kuni. Brachial plexus injury: clinical manifestations, conventional imaging findings, and the latest imaging techniques. Radiographics 2006;26:S133–43.

(18) Kline DG. Surgical repair of brachial plexus injury. J Neurosurg 2004;101:361–4.

(19) Sujay Sheth BA, Barton F, Branstetter IV, Edward J Escott. Appearance of normal cranial nerves on steady-state free precession MR images. Radiographics 2009;29:1045–55.

(20) Hayashi N, Masumoto T, Abe O, Aoki S, Ohtomo K, Tajiri Y. Accuracy of abnormal paraspinal muscle findings on contrast-enhanced MR images as indirect signs of unilateral cervical root-avulsion injury. Radiology 2002;223:397–402.

(21) Linda Dorota Dominika, Harish Srinivasan, Stewart Brian G, Parasu Naveen, Rebelo Ryan Paul. Multimodality imaging of peripheral neuropathies of the upper limb and brachial plexus. Radiographics 2010;30:1373–400.

(22) Doi K, Otsuka K, Okamoto Y, et al.. Cervical nerve root avulsion in brachial plexus injuries: magnetic resonance imaging classification and comparison with myelography and computerized tomography myelography. J Neurosurg 2002;96:277–84.

(23) Chavhan Govind B, Babyn Paul S, Jankharia Bhavin G, Cheng Hai-Ling M, Shroff Manohar M. Steady-state MR imaging sequences: physics, classification, and clinical applications. Radiographics 2008;28:1147–60.

(24) Mugler III JP. Basic principles. In: Edelman RR, Hesselink JR, Zlatkin MB, Crues JV, editors. Clinical magnetic resonance imaging. Philadelphia, PA: Saunders Elsevier; 2006. p. 23–57.

(25) Scheffler K, Lehnhardt S. Principles and applications of balanced SSFP technique. Eur Radiol 2003;13:2409–18.

(26) Carroll TJ, Sakaie KE, Wielopolski PA, Edelman RR. Advanced imaging techniques, including fast imaging. In: Edelman RR, Hesselink JR, Zlatkin MB, Crues JV, editors. Clinical magnetic resonance imaging. Philadelphia, PA: Saunders Elsevier; 2006. p. 187–230.

(27) Absil J, Denolin V, Metens T. Fat attenuation using a dual steady-state balanced-SSFP sequence with periodically variable flip angles. Magn Reson Med 2006;55:343–51.

(28) Van Ouwerkerk WJ, Strijers RL, Barkhof F, Umans U, Vandertop WP. Detection of root avulsion in the dominant C7 obstetric brachial plexus lesion: experience with three-dimensional constructive interference in steady-state magnetic resonance imaging and electrophysiology. Neurosurgery 2005;57(5):930–40.

(29) Sheth Sujay, Branstetter IV Barton F, Escott Edward J. Appearance of normal cranial nerves on steady-state free precession MR images. Radiographics 2009;29:1045–55.

(30) Zhou Lan, Yousem David M, Chaudhry Vinay. FRCPI: role of magnetic resonance neurography in brachial plexus lesions. Muscle Nerve 2004;30:305–9.